Finite Element and Analytical Modelling of Ship Unloader

Zrnić Nenad[1*], Gašić Vlada[1], Urošević Marko[1], Arsić Aleksandra[1]
[1]Faculty of Mechanical Engineering, Department of Material Handling Constructions and Logistics, University of Belgrade, Belgrade (Serbia)

The paper deals with the mathematical modelling of the dynamic behaviour of the structure of the ship unloader. It is given the procedure for formulation of the reduced dynamic model which retains the main aspects of the behaviour of the structure and yet is simple enough to be performed with standard engineering tools. The approach is applied on the real bridge-type grab ship unloader but can also be used on similar complex structures. Initially, the complete structure is modelled with finite element software where the natural frequencies were obtained. This 3D model is reduced to an equivalent plane model of the sea-side part of the boom. The postulation of the analytical approach is based on the model of a simple beam with an overhang where dynamic analysis is concerned with the Rayleigh Ritz method for estimating the adopted admissible functions. The results of the modal analysis of the reduced mathematical model showed a small difference from the results of finite element analysis which stands for the verification of the presented approach.

Keywords: Ship unloader, FEM analysis, Mathematical modelling

1. INTRODUCTION

Ship unloaders are machines located in ports and docks to facilitate bulk material exportation. These cranes are used to transfer, continually, solid bulk material from the ship to the shore and conversely such as iron ore, coal, fertilizers, and grains.

Over time, from 1959 [1] until today, the size, mass, and strength of the crane structures have increased due to the increasing size of ships and the constant growth of goods traffic in ports. However, the structures of the cranes remained relatively slender, i.e. their stiffness did not increase proportionally. Therefore, the movement of the trolley over the boom, as well as the lifting of the grab with material, can cause unacceptable deflection of the structure, especially in the vertical plane, [2]. According to these facts, the dynamic analysis is necessary in process of projecting in order to prevent the occurrence of unwanted stress states and deformations that can greatly reduce the productivity of these systems.

A detailed numerical analysis of the moving load problem for the lifting boom of a ship unloader is given in [3,4]. To analyze the dynamic response of the crane boom structure due to moving mass, the first step should be to create a reliable finite element (FE) model which will give corresponding natural frequencies and the vibration mode shapes of the crane structure, [5].

Creating a mathematical model plays an important role when it is impossible to perform experimental analyzes of the dynamic behaviour of the structure, and can also enable the optimization of the structure by varying the design parameters of the crane while maintaining maximum utilization of its capacity, [6].

In this paper, a numerical and mathematical model of the real construction of a ship unloader for obtaining its natural frequencies is developed. It is a project of the company Ceretti Tanfani S.p.A. Milano [7] for the needs of the Port of Bar. The construction of the boom is made of two girder (double girder boom) and box cross-section, which is connected to the pillar with one forestay and one backstay. Main technical characteristics of this crane is given in Table 1.

Table 1: Main technical characteristics of observed ship unloader

Capacity, (Q)	$400\ t/h$
Maximum load capacity, (M)	$12\ t$
Lifting height above the rail level, (H_1)	20 m
Reach from water side leg, (L_w)	32 m
Reach from land side leg, (L_l)	26 m
Span between the legs, (L_s)	28 m
Width between the legs, (B)	$14\ m$
Total height, (H)	≈ 51 m

2. NUMERICAL MODEL

In order to perform a modal analysis of the mathematical model of the ship unloader, it is necessary to form its numerical model on the basis of which the natural frequencies will be obtained, which will later be used to verify the results of the mathematical model.

Initially, a 3D FE model – Model 1 of the entire crane was developed (Figure 1). This model is used as a reference for the verification of reduced numerical models. The values of natural frequencies of the structure for the first five modes are given in Table 2.

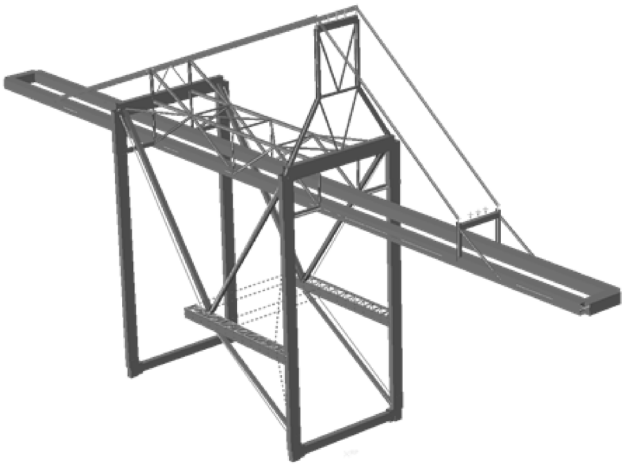

Figure 1: View of the Model 1

*Corresponding autor: University of Belgrade, FME, Kraljice Marije 16, 11120 Belgrade, Serbia, nzrnic@mas.bg.ac.rs

Table 2: Values of the natural frequencies for the first five modes

MODES	Frequencies [Hz]	Periods [s]
I	0.5308	1.8839
II	0.6049	1.6532
III	1.108	0.9025
IV	1.7362	0.576
V	2.1569	0.4636

Figure 2 shows that in the fifth mode, the boom vibrates practically independently from other parts of the structure. Based on this the part of the boom on the waterside leg can be adopted as a representative to describe the behavior of the entire crane structure, [8].

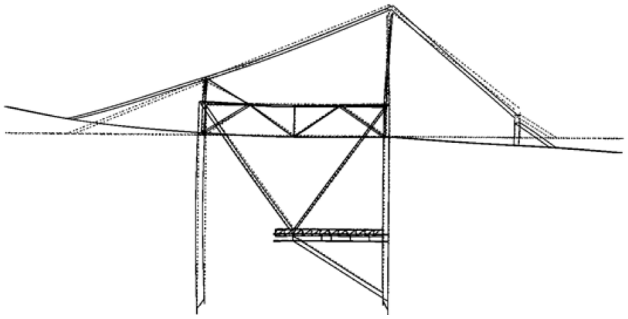

Figure 2: The fifth mode of the vibration of the ship unloader

According to the previous assumption Model 2 was created as an equivalent 2D, non-linear FE model of the boom from the hinge to its end and forestay (Figure 3). Support A is modelled as a hinge and represents the real connection between the boom and the rest of the structure. Table 3 gives all the geometric and physical characteristics of Model 2.

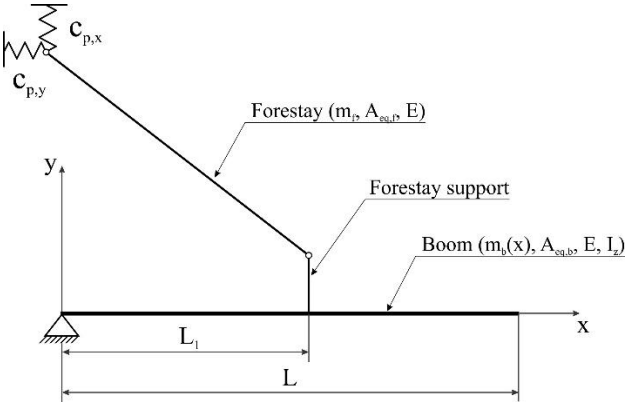

Figure 3: Equivalent 2D FE model of the ship unloader – Model 2

In Figure 1 it can be seen that the stiffness of the pillar in the horizontal and vertical directions is not negligible, so it is taken into account in Model 2 through the springs of the corresponding equivalent stiffnesses $c_{p,x}$ and $c_{p,y}$. By introducing external unit loads (force $\bar{F}$) into the corresponding nodes of Model 1, the displacements of the structure δ_{p,x_1}, δ_{p,y_1} and δ_{p,x_2}, δ_{p,y_2} in the corresponding directions were obtained. By calculating the arithmetic values (1) and (2) of the obtained displacements, the stiffness values $c_{p,x}$ and $c_{p,y}$ (3) and (4) were determined.

$$\delta_{p,x} = \frac{\delta_{p,x_1} + \delta_{p,x_2}}{2} = 6.9351902 \cdot 10^{-8}\ \text{m} \tag{1}$$

$$\delta_{p,y} = \frac{\delta_{p,y_1} + \delta_{p,y_2}}{2} = 6.32639674 \cdot 10^{-9}\ \text{m} \tag{2}$$

$$c_{p,x} = \frac{\bar{F}}{\delta_{p,x}} = 14419200\,\frac{\text{N}}{\text{m}} \tag{3}$$

$$c_{p,y} = \frac{\bar{F}}{\delta_{p,y}} = 158067900\,\frac{\text{N}}{\text{m}} \tag{4}$$

Table 3: Geometric and physical characteristics of Model 2

Boom length, (L)	34.13 m
Distance from support A to support of the forestay, (L_1)	18.464 m
Forestay length, (L_f)	25.025 m
Equivalent mass per unit meter of the boom, $(m_b(x))$	$1007\ \frac{kg}{m}$
Equivalent mass of the forestay, (m_f)	$4010\ kg$
Young's modulus of elasticity, (E)	$2.1 \cdot 10^{11}\ \frac{\text{N}}{\text{m}^2}$
Equivalent section area of the boom, $(A_{eq,b})$	$0.09504\ \text{m}^2$
Equivalent section area of the forestay, $(A_{eq,f})$	$0.01562\ \text{m}^2$
Equivalent axial moment of inertia of the boom, (I_z)	$0.0207498\ \text{m}^4$

The next reduction is the approximation of the forestay by a spring (Model 3) which stiffness is determined by the characteristics of the forestay geometry (5). The forestay mass is reduced to the points of its supports. Model 3 is shown in Figure 4.

$$c_f = \frac{E \cdot A_{eq,f}}{L_f} = 131076923{,}1\,\frac{\text{N}}{\text{m}} \tag{5}$$

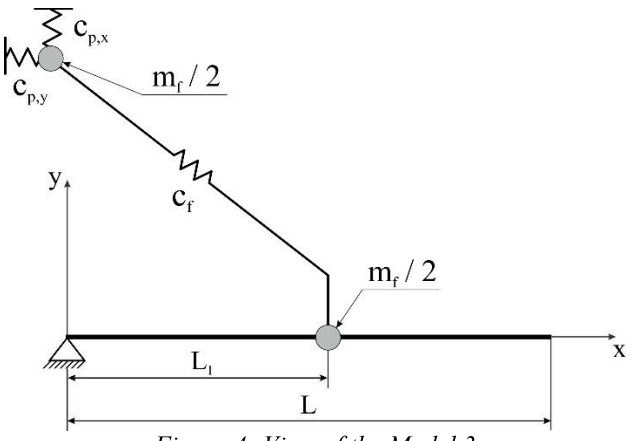

Figure 4: View of the Model 3

Model 4 (Figure 5) is a model in which a three-spring system is replaced by a single spring of equivalent stiffness. Since the stiffness of the springs is a characteristic of the system and does not depend on the mass and stiffness of the boom and the mass of the forestay, all masses are neglected, while the stiffness of the boom is taken as an infinite value. By entering the unit load in the direction of the forestay, the displacement in the same direction $\delta_{f,F}$ is obtained, on the basis of which the values of equivalent stiffness $c_{1,eq}$ can be determined by (6).

$$c_{1,eq} = \frac{\bar{F}}{\delta_{f,F}} = 18773134.72\,\frac{\text{N}}{\text{m}} \tag{6}$$

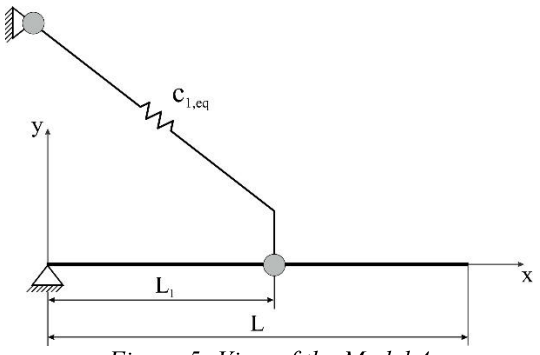

Figure 5: View of the Model 4

Model 5 is a reduced model in which the spring with the stiffness $c_{1,eq}$ is divided into two springs with the stiffnesses $c_{1,eq,x}$ and $c_{1,eq,y}$ in the horizontal and vertical directions, respectively. The concentric mass of the forestay in the upper support is neglected, which is shown in Figure 6. The procedure for determining the stiffnesses of the new springs is the same as in Model 4, while their numerical values are determined according to:

$$c_{1,eq,x} = \frac{\bar{F}_{c_1,x}}{|\delta_{31} \cdot sin\,\alpha - \delta_{21} \cdot cos\,\alpha|} = 50760449.52\frac{N}{m} \quad (7)$$

$$c_{1,eq,y} = \frac{\bar{F}_{c_1,y}}{|\delta_{31} \cdot cos\,\alpha + \delta_{21} \cdot sin\,\alpha|} = 9181334.46\frac{N}{m} \quad (8)$$

where $\bar{F}_{c_1,x}$ is projection of the force in the spring on the x-axis, $\bar{F}_{c_1,y}$ is projection of the force in the spring on the y-axis, $\delta_{31} \cdot \sin\alpha$ is projection of the corresponding displacement perpendicular on the forestay direction on the x-axis, $\delta_{21} \cdot \cos\alpha$ is projection of the corresponding displacement parallel on the forestay direction on the x-axis, $\delta_{31} \cdot \cos\alpha$ is projection of the corresponding displacement perpendicular on the forestay direction on the y-axis, $\delta_{21} \cdot \sin\alpha$ is projection of the corresponding displacement parallel on the forestay direction on the y-axis and α is an angle between forestay and boom.

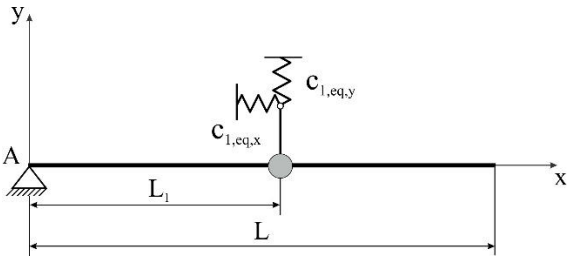

Figure 6. View of the Model 5

By applying a unit force $\bar{F}$ in the vertical direction at support B, the displacement in the same direction δ_v is obtained. This reduces the system of two springs to one equivalent spring whose stiffness c_{eq} is determined according to (9). The newly made system - Model 6 is shown in Figure 7.

$$c_{eq} = \frac{\bar{F}}{\delta_v} = 11900399.16\frac{N}{m} \quad (9)$$

Model 6 represents a beam with an overhang of total length $L = 34.1$ m whose left support A presents a cylindrical joint while at a distance of $L1 = 18.5$ m it is supported by a vertical spring. $M_1 = 8695$ kg is lumped mass originating from the forestay weight and forestay support construction. The boom is modelled as a system with distributed mass where m_b is mass per unit length and EI_z is the flexural rigidity of the boom structure.

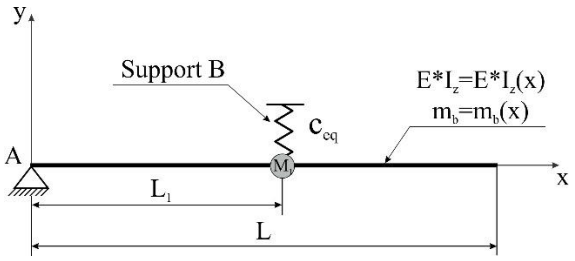

Figure 7: View of the Model 6

Model 2 - Model 6 were verified by comparing the obtained oscillation period of the first mode in the vertical direction with the corresponding mode of Model 1 (mode V from the Table 2). Oscillation period values and relative deviations are shown in Table 4, where relative deviations are obtained according to:

$$\left|\frac{T_n - T_1}{T_1}\right| \cdot 100\%, \quad n = 2,3,4,5,6. \quad (10)$$

where T_n is oscillation period of corresponding reduced numerical model and T_1 is oscillation period of Model 1.

Table 4: Comparative table of values of the oscillation period for the first mode of oscillation in the vertical plane

Model	Period [s]	Dev. [%]
2	0.4405	4.98
3	0.4405	4.98
4	0.4363	5.89
5	0.432	6.81
6	0.48	3.54

As can be seen from Table 4, the relative deviations are acceptable from the aspect of engineering accuracy on the basis of which Model 6 can be adopted as a reference model for forming a mathematical model of ship unloader.

The first mode in the vertical plane of Model 6 is shown in Figure 8, while the higher frequency modes are shown in Figures 9-12.

Figure 8: First mode in vertical plane – Model 6, $f = 2.0926\ Hz$, $T = 0.48\ s$

Figure 9: Second mode, $f = 4.8963\ Hz$, $T = 0.2042\ s$

Figure 10: Third mode, $f = 13.854\ Hz$, $T = 0.0722\ s$

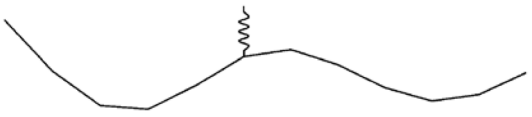

Figure 11: Fourth mode, $f = 27.357\ Hz$, $T = 0.0365\ s$

Figure 12: Fifth mode, $f = 46.31\ Hz$, $T = 0.0216\ s$

3. MATHEMATICAL MODEL

As the system shown in Figure 6 is not a "classical" system whose ready-made analytical solutions can be found in the literature, it is necessary to use one of the approximate methods for determining the natural frequencies of the model. In the following text, the procedure for solving this problem using the Rayleigh-Ritz method will be presented.

The Rayleigh-Ritz method is based on solving the equation of the form (11), which also represents the function of moving the points on the structure.

$$y_n(x) = \sum_{i=1}^{n} a_i \cdot \emptyset_i \tag{11}$$

In (11) $a_1, a_2, \dots, a_n$ are unknown coefficients determined from the boundary conditions, and $\emptyset_1, \emptyset_2, \dots, \emptyset_n$ represent n linearly independent admissible functions. By this procedure, a continuous system with an infinite number of degrees of freedom (DoF) is reduced to a discretized system with n DoF.

The Rayleigh-Ritz method is an extension of the Rayleigh method which determines the fundamental frequency of the system. In the first approximation, the Rayleigh method can adopt a test admissible function in the form $\emptyset_1(x) = \frac{x}{L}$ which represents the upper limit of the first eigenvalue, as shown in [9]. In the next approximation, the Rayleigh-Ritz method performed an additional reduction of the obtained value of the basic function as well as the formation of a test function that is sufficiently close to the form of the first mode of oscillation of the adopted mathematical model.

The determination of higher frequencies of the system is based on the definition of additional permissible functions, which reduces the system to a system with a finite number of DoF. According to [10] from an engineering point of view the number of 5 admissible functions describes the dynamic behavior of the system with sufficient accuracy.

After several iterations, the admissible functions that satisfy all geometric boundary conditions were adopted, while some of them also satisfy the natural boundary conditions in the left support A of the boom and have the following shape:

$$\emptyset_1(x) = \frac{x}{L} \tag{12}$$

$$\emptyset_2(x) = sin\frac{\pi x}{L} \tag{13}$$

$$\emptyset_3(x) = sin\frac{2\pi x}{L} \tag{14}$$

$$\emptyset_4(x) = sin\frac{3\pi x}{L} \tag{15}$$

$$\emptyset_5(x) = sin\frac{4\pi x}{L} \tag{16}$$

It can be shown that the coefficients of mass and stiffness are obtained through the kinetic and potential energy of the system in the form:

$$m_{ij} = \int_0^L m_b \phi_i(x)\phi_j(x)\,dx + M_1\phi_i(L_1)\phi_j(L_1) \tag{17}$$

$$c_{ij} = \int_0^L EI_z \frac{\partial^2\phi_i(x)}{\partial x^2}\frac{\partial^2\phi_j(x)}{\partial x^2}dx + c_{eq}\phi_i(L_1)\phi_j(L_1) \tag{18}$$

For the specific values of the parameters from Table 3, the following coefficients of mass and stiffness were obtained and presented in matrix form:

$$M = \begin{bmatrix} 1.401\cdot10^4 & 1.561\cdot10^4 & -6.669\cdot10^3 & -709.282 & -421.673 \\ 1.561\cdot10^4 & 2.574\cdot10^4 & -2.194\cdot10^3 & -7.989\cdot10^3 & 4.243\cdot10^3 \\ -6.669\cdot10^3 & -2.194\cdot10^3 & 1.776\cdot10^4 & 2.05\cdot10^3 & -1.089\cdot10^3 \\ -709.282 & -7.989\cdot10^3 & 2.05\cdot10^3 & 2.466\cdot10^4 & -3.964\cdot10^3 \\ -421.673 & 4.243\cdot10^3 & -1.089\cdot10^3 & -3.964\cdot10^3 & 1.93\cdot10^4 \end{bmatrix} \tag{19}$$

$$C = \begin{bmatrix} 3.482\cdot10^6 & 6.384\cdot10^6 & -1.638\cdot10^6 & -5.964\cdot10^6 & 3.168\cdot10^6 \\ 6.384\cdot10^6 & 1.704\cdot10^7 & -3.003\cdot10^6 & -1.093\cdot10^7 & 5.808\cdot10^6 \\ -1.638\cdot10^6 & -3.003\cdot10^6 & 8.616\cdot10^7 & 2.805\cdot10^6 & -1.49\cdot10^6 \\ -5.964\cdot10^6 & -1.093\cdot10^7 & 2.805\cdot10^6 & 4.425\cdot10^8 & -5.426\cdot10^6 \\ 3.168\cdot10^6 & 5.808\cdot10^6 & -1.49\cdot10^6 & -5.426\cdot10^6 & 1.369\cdot10^9 \end{bmatrix} \tag{20}$$

The solution of the frequency equation has the form:

$$\Lambda = \omega^2 \tag{21}$$

where ω is a circular frequency and has a shape:

$$\omega = \sqrt{\frac{c_{ij}}{m_{ij}}} \tag{22}$$

By further calculation, the following concrete values were obtained for the first five circular frequencies ω [s^{-1}], natural frequencies f [Hz] and eigenperiods T [s]:

$$\omega = \begin{bmatrix} 12.921 \\ 30.006 \\ 84.672 \\ 176.348 \\ 310.909 \end{bmatrix},\quad f = \begin{bmatrix} 2.056 \\ 4.776 \\ 13.476 \\ 28.067 \\ 49.483 \end{bmatrix},\quad T = \begin{bmatrix} 0.486292 \\ 0.209395 \\ 0.074206 \\ 0.03563 \\ 0.020209 \end{bmatrix} \tag{23}$$

Eigenvectors which also represent the coefficients a_1, a_2, a_3, a_4, a_5 have the values:

$$EGV1 = \begin{bmatrix} -0.96 \\ 0.28 \\ 3.03\cdot10^{-3} \\ -6.679\cdot10^{-3} \\ 1.211\cdot10^{-3} \end{bmatrix} \tag{24}$$

$$EGV2 = \begin{bmatrix} 0.628 \\ -0.777 \\ -0.05 \\ 1.152\cdot10^{-3} \\ -5.23\cdot10^{-4} \end{bmatrix} \tag{25}$$

$$EGV3 = \begin{bmatrix} -0.685 \\ 0.355 \\ -0.629 \\ -0.094 \\ 0.016 \end{bmatrix} \tag{26}$$

$$EGV4 = \begin{bmatrix} 0.691 \\ -0.517 \\ 0.284 \\ -0.415 \\ -0.048 \end{bmatrix} \tag{27}$$

$$EGV5 = \begin{bmatrix} -0.691 \\ 0.506 \\ -0.249 \\ 0.116 \\ -0.437 \end{bmatrix} \tag{28}$$

By substituting the specific values of the coefficients a_1 - a_5 as well as the adopted admissible functions in (11), the following functions $y_n(x)$ are obtained:

$$y_1(x) = -0.96 \cdot \frac{x}{L} + 0.28 \cdot \sin\frac{\pi x}{L} + 3.03 \cdot 10^{-3} \cdot \sin\frac{2\pi x}{L} - 6.679 \cdot 10^{-3} \cdot \sin\frac{3\pi x}{L} + 1.211 \cdot 10^{-3} \cdot \sin\frac{4\pi x}{L} \quad (29)$$

$$y_2(x) = 0.628 \cdot \frac{x}{L} - 0.777 \cdot sin\frac{\pi x}{L} - 0.05 \cdot sin\frac{2\pi x}{L} + 1.152 \cdot 10^{-3} \cdot sin\frac{3\pi x}{L} - 5.23 \cdot 10^{-4} \cdot sin\frac{4\pi x}{L} \quad (30)$$

$$y_3(x) = -0.685 \cdot \frac{x}{L} + 0.355 \cdot sin\frac{\pi x}{L} - 0.629 \cdot sin\frac{2\pi x}{L} - 0.094 \cdot sin\frac{3\pi x}{L} + 0.016 \cdot sin\frac{4\pi x}{L} \quad (31)$$

$$y_4(x) = 0.691 \cdot \frac{x}{L} - 0.517 \cdot sin\frac{\pi x}{L} + 0.284 \cdot sin\frac{2\pi x}{L} - 0.415 \cdot sin\frac{3\pi x}{L} - 0.048 \cdot sin\frac{4\pi x}{L} \quad (32)$$

$$y_5(x) = -0.691 \cdot \frac{x}{L} + 0.506 \cdot sin\frac{\pi x}{L} - 0.249 \cdot sin\frac{2\pi x}{L} + 0.116 \cdot sin\frac{3\pi x}{L} + -0.437 \cdot sin\frac{4\pi x}{L} \quad (33)$$

4. RESULTS AND DISCUSSION

The oscillation forms of the mathematical model of the ship unloader obtained by the Rayleigh-Ritz method are presented in Figure 13.

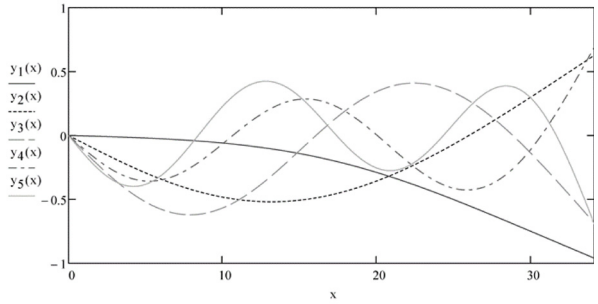

Figure 13: The first five modes of vibration obtained by Rayleigh-Ritz method

Values of eigenperiods for the first five modes of oscillation in the vertical plane obtained by the Rayleigh-Ritz method (23) were verified by their comparing with corresponding periods from the numerical results of FE Model 6 (Figures 8 - 12). Their percentage deviations are given in Table 5, while Figures 14-18 present the graphical comparisons of the corresponding modes of vibration.

Table 5: Percentage deviations of the eigenperiods of Model 6 and mathematical model

MODES	Eigenperiods [s]		Dev.
	Math. model	Model 6	[%]
I	0.486292	0.48	1.31
II	0.209395	0.2042	2.54
III	0.074206	0.0722	2.78
IV	0.03563	0.0365	2.38
V	0.020209	0.0216	6.44

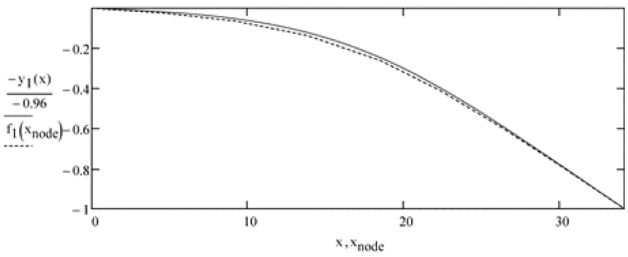

Figure 14: Comparison of the normalized first mode of vibration of the mathematical and FE model

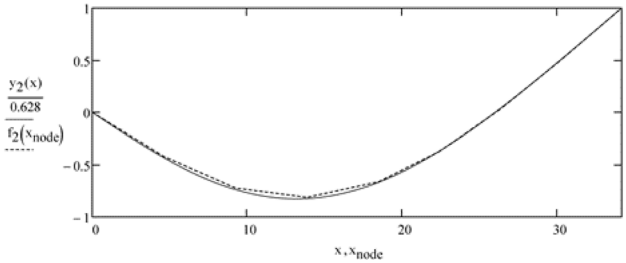

Figure 15: Comparison of the normalized second mode of vibration of the mathematical and FE model

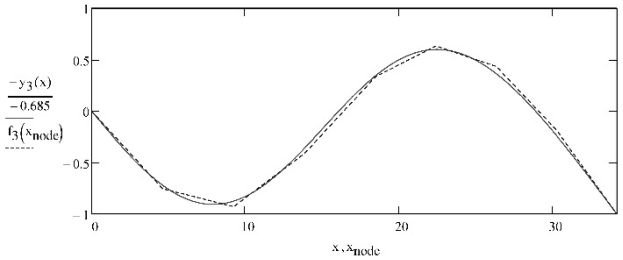

Figure 16: Comparison of the normalized third mode of vibration of the mathematical and FE model

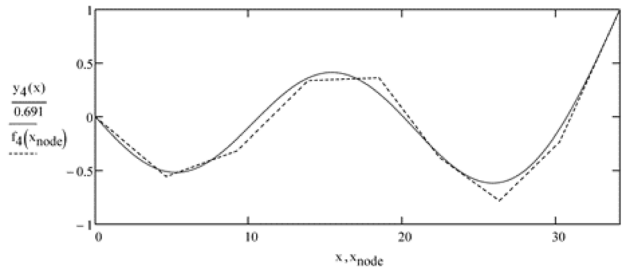

Figure 17: Comparison of the normalized fourth mode of vibration of the mathematical and FE model

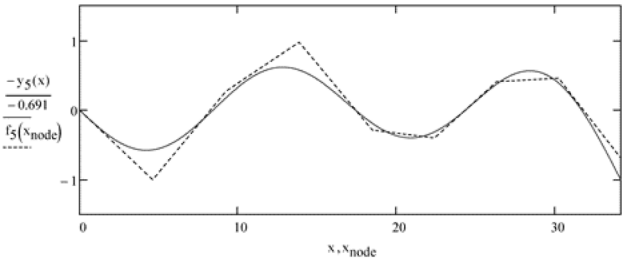

Figure 18: Comparison of the normalized fifth mode of vibration of the mathematical and FE model

As can be observed in Figures 14 - 18, there is very good matching of the first three normalized modes of oscillation between mathematical and numerical model, while slightly larger deviations occur only in the fourth and fifth modes. This shows that the adopted admissible functions can be considered as a sufficiently accurate approximation of the real eigenfunctions of the dynamical system and that the number of 5 adopted admissible functions is sufficient to obtain reliable results from the aspect of engineering accuracy.

5. CONCLUSION

Given that this type of construction is not widely used as, e.g. overhead traveling cranes, the dynamic problems that occur during their exploitation are still not sufficiently examined and discussed in the available literature. The aim of this paper was to present the procedure of modal analysis which gives the first insights into the dynamic behaviour of the structure and as such can be used already in the design phase of these structures.

The paper shows that the complex structure of a ship unloader can be reduced to a relatively simple 2D

system of a beam with an overhang, supported on one fixed and one elastic support, while completely preserving the nature of the behaviour of the real structure. As can be seen from Table 4 and Table 5 numerically and mathematically calculated results are in very close agreement which means that the presented approach can be considered acceptable from the aspect of engineering accuracy.

The mathematical model formed in this way can be used as a basis for further analysis of dynamics problems that occur on structures of this type (moving load problem, fatigue, etc.).

ACKNOWLEDGEMENTS

This work is a result of research supported by the Ministry of Education, Science and Technological Development of the Republic of Serbia by Contract 451-03-68/2020-14/200105.

REFERENCES

[1] N. Zrnić and K. Hoffmann, “Development of design of ship-to-shore container cranes: 1959-2004”, History of Machines and Mechanisms, C. Marco, ed., Kluwer Academic Publishers, Dodrecht, pp. 229–242, (2004)

[2] N. Zrnić, D. Oguamanam and S. Bošnjak, “Dynamics and modelling of mega quayside container cranes”, FME Trans., Vol. 34, pp. 193–198, (2006)

[3] M. Giulia, K. Banisoleiman and A. Gonzalez, “An investigation into the moving load problem for the lifting boom of a ship unloader”, Eng. Struct., Vol. 234, pp. 1–20, (2021)

[4] M. Giulia, K. Banisoleiman and A. Gonzalez, “Impact of a moving trolley on the dynamic response of a ship unloader boom”, 13th International Conference on Steel, Space and Composite Structures (SS18), Perth (Australia), 31 January-2 February 2018, pp. 33-38, (2011)

[5] D. Dinevski, M. Oblak and A. Novak, “Experimental verification of the container crane natural frequencies”, Transactions on Modelling and Simulations, Vol. 16, WIT Press, pp. 245-254, (1997)

[6] N. Zrnić, K. Hoffmann and S. Bošnjak, “Modelling of dynamic interaction between structure and trolley for mega container cranes”, Math. Comput. Model. Dyn. Syst., Vol. 15, pp. 295–311, (2009)

[7] Ceretti Tanfani S.p.A. Milano, Ship unloader 400 t/h, (1982)

[8] N. Zrnić, S. Bošnjak and K. Hoffmann, “Parameter sensitivity analysis of non-dimensional models of quayside container cranes”, Math. Comput. Model. Dyn. Syst., Vol. 16, pp. 145–160, (2010)

[9] N. Zrnić, “Uticaj kretanja kolica na dinamičko ponašanje obalskih kontejnerskih dizalica”, PhD Thesis, University of Belgrade (Serbia), (2005)

[10] R.L. Clark, W.R. Saunders and G.P. Gibbs, “Adaptive Structures: Dynamics and Control”, John Wiley & Sons, New York (US), (1998)